Electrically tunable electron spin lifetimes in GaAs(111)B quantum wells

K. Biermann, A. Hernández-Mínguez, R. Hey, and P. V. Santos

Citation: J. Appl. Phys. **112**, 083913 (2012); doi: 10.1063/1.4759241
View online: http://dx.doi.org/10.1063/1.4759241
View Table of Contents: http://jap.aip.org/resource/1/JAPIAU/v112/i8
Published by the American Institute of Physics.

Electrically tunable electron spin lifetimes in GaAs(111)B quantum wells

K. Biermann,[a] A. Hernández-Mínguez, R. Hey, and P. V. Santos
Paul-Drude-Institut für Festkörperelektronik, Hausvogteiplatz 5-7, 10117 Berlin, Germany

(Received 1 August 2012; accepted 19 September 2012; published online 19 October 2012)

We investigate the electric tunability of the electron spin lifetime in GaAs(111) quantum wells (QWs) inserted in biased p-i-n and n-i-p diode-like structures. Due to the specific symmetry of these QWs, the Rashba contribution to the spin-orbit magnetic field induced by the applied bias is parallel to the intrinsic Dresselhaus contribution for all directions of the electron wavevector. In particular, the voltage applied to the diode, which controls the amplitude of the Rashba contribution, can be adjusted to attenuate the resulting spin-orbit field, thus strongly suppressing spin dephasing due to the Dyakonov-Perel relaxation mechanism for all spin orientations. Spin lifetimes from below 100 ps at an electric field of −20 kV/cm to values exceeding 4 ns at +8 kV/cm have been measured in 25 nm thick multiple QWs at a temperature of 20 K. © *2012 American Institute of Physics*. [http://dx.doi.org/10.1063/1.4759241]

I. INTRODUCTION

Spintronics devices for future semiconductor integrated circuits require efficient techniques for the electrical injection and transport of spins as well as for their detection and manipulation. In this respect, one of the main challenges is the achievement of spin lifetimes sufficiently long to permit the realization of many spin operations before decoherence effects set in. This problem becomes specially important when one takes into account that the electron spin coherence times in intrinsic III-V bulk semiconductors are of the order of only one ns.

Three classes of spin scattering mechanisms dominate the electron spin lifetime of semiconductor structures. The first is the spin-orbit (SO) interaction, which couples the spins to the orbit degree of freedom of the carriers. This interaction induces a spin splitting of the conduction bands, which depends on the magnitude and direction of the electron wavevector $\mathbf{k}$. The effect of the SO interaction on the electron spin dynamics can be described in terms of an effective magnetic field ($\mathbf{B}_{so}$) acting on moving spins. As a result, electrons in an ensemble with different $\mathbf{k}$ experience SO fields of different strengths and directions. Their spins will then precess at different rates, leading to a reduction of the resulting ensemble spin. This is known as the Dyakonov-Perel (DP) spin dephasing mechanism.[1–3] The SO interaction can also couple different spin states during electron scattering processes. One example is the Elliott-Yafet spin dephasing mechanism,[4] which describes spin-flip transitions induced during electron scattering by impurities or phonons and is expected to be influential in highly doped, low-bandgap materials. A second example is the intersubband spin relaxation mechanism[5] in quantum well (QW) structures, where electron scattering between two subbands is accompanied by a spin flip. This mechanism depends on the occupation probability of the upper subband and is thus expected to be negligible at low temperature and low concentrations of free electrons.

The second class of spin scattering processes is associated with electron spin flips mediated by the electron-hole exchange interaction, the so-called Bir-Aronov-Pikus (BAP) spin dephasing mechanism.[6] This mechanism becomes important for excitons[7] as well as in highly p-type doped III-V semiconductors at low temperatures.[8] The last class of scattering processes arises from the hyperfine-interaction between carrier and nuclear spins. The associated spin flip probability is normally negligible for free carriers, but becomes important for localized electrons in quantum dots.

From the mechanisms presented above, the BAP and DP spin dephasing processes represent the most severe processes limiting the electron spin lifetime in undoped GaAs QWs. While the former can be minimized by spatially separating electrons and holes, two types of strategies have been developed during the last years to reduce the impact of DP relaxation on the spin lifetime. The first relies on the fact that the DP spin scattering rate is inversely proportional to the momentum scattering rate:[1] Frequent momentum scattering reduces the effective SO field $\mathbf{B}_{so}$ experienced by the electrons spins, thus leading to longer lifetimes. One approach consists in the introduction of moderate levels of n-type dopants in QW structures. While suppressing the BAP scattering by reducing the hole concentration, the frequent scattering on the dopants randomizes $\mathbf{B}_{so}$, thus increasing the spin lifetimes to several tens of ns.[9,10] The introduction of dopants, however, makes it difficult to control the spin density to very small levels (down to single spins). An alternative approach employs a confinement potential to control the SO interaction: Here, the frequent carrier reflections at the borders of the potential replace the scattering dopants.[11] In particular, the use of one-dimensional potentials or of moving potential dots enables the simultaneous confinement and transport of spins over large distances.[12–15]

The second strategy to reduce DP dephasing exploits the dependence of the SO interaction in QW structures on crystallographic orientation, a topic which will be discussed in detail in Sec. II. As an example, the specific symmetry of (110)GaAs QWs[3] has been successfully exploited to achieve lifetimes exceeding 20 ns for electron spins aligned along the QW growth directions.[16–18] One limitation of this approach

[a]Author to whom correspondence should be addressed. Electronic mail: biermann@pdi-berlin.de.

is that the long lifetime only applies to spins along the growth direction. As the spins are rotated away from the [110] axis, spin dephasing becomes strongly enforced by the DP mechanism,[19,20] thus severely hampering spin manipulation. A more promising approach, which will be subject of the present paper, takes advantage of the compensation of the bulk (BIA) and the structural inversion asymmetry (SIA) contribution to the SO interaction in QWs grown along the [111] axis. The compensation can be achieved by applying an electric field to control the SIA contribution. In this case, electron spin lifetimes and precession rates are expected to be electrically controllable with values independent of the spin orientation and propagation direction. This special property of (111) III-V structures, which is discussed in details in Sec. II, has been predicted[21–23] and recently experimentally demonstrated by Balocchi *et al.*[24] A further advantage of the compensation approach is that the vertical (i.e., along the growth direction) electric field also minimizes BAP scattering by reducing overlap between the electron and the hole wave functions.

In this work, we present a detailed study of the spin dynamics in multiple (111) GaAs QWs (MQWs) under a vertical electric field. The experimental studies were carried out at 20 K in MQW structures consisting of 25 nm-thick QWs embedded within the intrinsic region of p-i-n and n-i-p diode structures. Time- and polarization-resolved photoluminescence (PL) measurements show a significant enhancement of the electron spin lifetime in n-i-p structures under increasing reverse bias. These results are in agreement with the findings of Ballochi *et al.*[24] in thinner (15 nm thick) QWs and are attributed to the partial compensation of the Dresselhaus and Rashba contributions to the spin-orbit interaction induced by the reverse bias. The lifetime enhancement persists while spins precess under an in-plane magnetic field. Time-resolved PL experiments carried out under these conditions show spin precession oscillations lasting over times exceeding 5 ns. Finally, the BIA-SIA compensation mechanism has been further corroborated by experiments on p-i-n structures, where the spin-orbit field increases under a reverse bias, thus leading to a significant reduction of the spin lifetime.

In Sec. II, we first address the different mechanisms controlling the SO interaction in QWs with different crystallographic directions. We then describe the procedures for the growth and processing (Sec. III) as well as for the spectroscopic measurements of the spin dynamics (Sec. IV). The experimental results are presented and discussed in Sec. V. Finally, concluding remarks are given in Sec. VI.

II. DEPENDENCE OF THE SPIN-ORBIT INTERACTION ON QUANTUM WELL SYMMETRY

As previously mentioned, there are two major contributions to the SO field in III-V QWs. The first one, denoted as $\mathbf{B}_{\mathrm{BIA}}$ (bulk inversion asymmetry) or as the Dresselhaus term, is of intrinsic nature and arises from the lack of inversion symmetry in III-V semiconductors. The second one is caused by an imposed asymmetry on the QW potential and is known as $\mathbf{B}_{\mathrm{SIA}}$ (structural inversion asymmetry) or Rashba term. The Rashba contribution can be induced by an asymmetrical doping profile or by an electric field applied across the QW. The directions of these SO fields in III-V QWs of various growth orientations are of particular interest since they crucially affect the dynamics of the electron spins. The panels in Fig. 1 depict the orientation of $\mathbf{B}_{\mathrm{BIA}}$ and $\mathbf{B}_{\mathrm{SIA}}$ as a function of the in-plane electron wavevector $\mathbf{k}_{\parallel} = (k_x, k_y)$ for (001), (110), and (111) QWs (the x and y directions for each QW orientation are indicated in the diagram). In these diagrams, and also throughout the article, we will only take into account terms of the SO interaction linear in the in-plane electron wavevector $\mathbf{k}_{\parallel}$.

In (001) QWs, both SO fields lie in the QW plane. For two distinct directions ($[\bar{1}10]$, $[110]$), $\mathbf{B}_{\mathrm{BIA}}$ and $\mathbf{B}_{\mathrm{SIA}}$ are aligned parallel to each other. For each of these directions, an external electric field can be used to make $\mathbf{B}_{\mathrm{SIA}} = -\mathbf{B}_{\mathrm{BIA}}$, thus compensating the total SO field.[25] However, this compensation simultaneously increases the total field for the orthogonal direction, thus leading to a strong in-plane anisotropy of spin lifetimes.[26–28]

The remarkable feature of the SO fields in (110) QWs is that $\mathbf{B}_{\mathrm{BIA}}$ is always normal to the QW plane. Therefore, electrons spins aligned along this direction—which is the typical

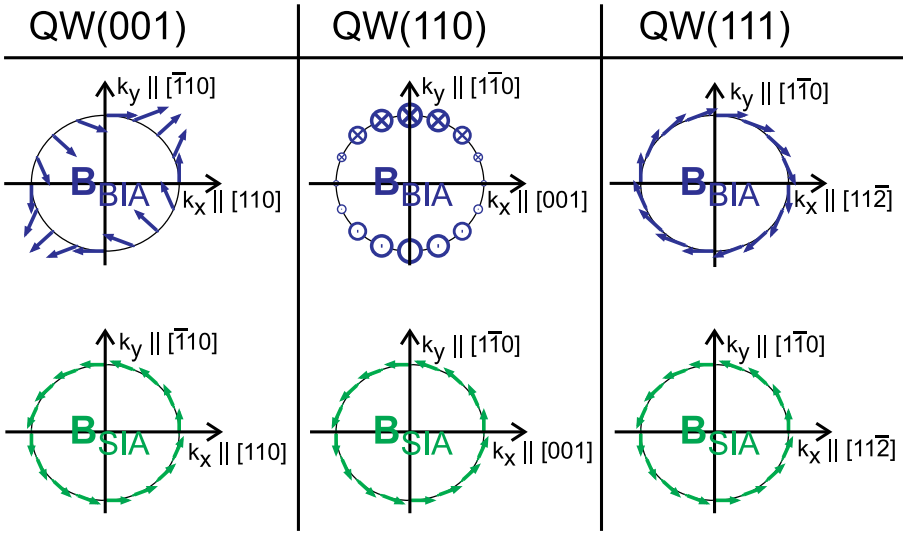

FIG. 1. Orientations of the spin-orbit magnetic fields associated with the bulk inversion asymmetry ($\mathbf{B}_{\mathrm{BIA}}(\mathbf{k})$) and with the structural inversion asymmetry ($\mathbf{B}_{\mathrm{SIA}}(\mathbf{k})$) fields in III-V QWs with (001), (110) and (111) orientations.

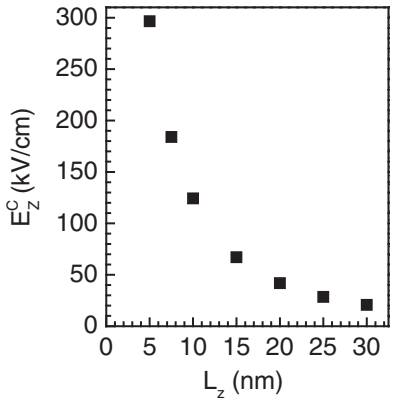

FIG. 2. Calculated compensation field strength E_Z^C [see Eq. (1)] as a function of the nominal QW width (L_Z). The table additionally lists the effective QW width (d_{eff}), which takes into account both the L_Z and the penetration of the electron wave functions into the QW barriers. The calculations were carried out using $\gamma = 17\,\text{eV Å}^3$ (Ref. 14) and $r_{41} = 4.15\,\text{e Å}^2$ (Ref. 32).

spin orientation for optical spin injection using circularly polarized light—will not be affected by $\mathbf{B}_{BIA}$. DP dephasing mechanism is thus suppressed for these spins, leading to long spin lifetimes.[3,6,18,29] An externally applied electric field can be very useful for "switching off" an existing out-of-plane spin polarization. In this case, the in-plane $\mathbf{B}_{SIA}$ generated by the electric field will rotate the spin vector, thus activating DP relaxation. Iba *et al.* used such a process to reduce the spin lifetime in (110) QWs by more than one order of magnitude by applying an electric field perpendicular to the QW plane.[19]

The specific symmetry of (111) QWs leads to the unique situation, where $\mathbf{B}_{BIA}$ and $\mathbf{B}_{SIA}$ are always parallel, independent of the electron wavevector. The total SO field ($\mathbf{B}_{BIA} + \mathbf{B}_{SIA}$) can, therefore, be minimized for all electron wavevectors by making $\mathbf{B}_{SIA} = -\mathbf{B}_{BIA}$.[21–23] The SO compensation condition is fulfilled for an electric field E_Z^C given by[21,30]

$$E_Z^C = \frac{1}{\sqrt{3}}\frac{\gamma}{r_{41}}\left(\frac{\pi}{d_{\text{eff}}}\right)^2 = \frac{1}{\sqrt{3}}\frac{2m^*}{\hbar^2}\frac{\gamma}{r_{41}}E_1. \qquad (1)$$

In this equation, m^* is the effective electron mass while γ and r_{41} denote the Dresselhaus and Rashba coefficients, respectively. For GaAs, γ was measured to be in the range $\gamma = 17 - 28\ \text{eV Å}^3$ (e ≡ electron charge).[14,31] For r_{41}, we use the value deduced in (110)GaAs QWs by Eldridge *et al.* of $4.15\,e\text{Å}^2$.[32] The effective QW thickness d_{eff} refers to the extension of the electron wave function, which depends on the nominal thickness of the QW (L_Z) and on the penetration into the barrier layers. On the right-hand-side of Eq. (1), d_{eff} is expressed in terms of the quantization energy of the lowest QW state (E_1).

Figure 2 displays the compensation field E_Z^C as a function of the nominal thicknesses (L_Z) of GaAs QWs with $Al_{0.2}Ga_{0.8}As$ barriers ranging from 5 to 30 nm as calculated from Eq. (1) using $\gamma = 17\,\text{eV Å}^3$ and $r_{41} = 4.15\,\text{eÅ}^2$.[32] The values of E_Z^C and the effective QW widths (d_{eff}) are also listed in the table next to the plot. Due to the inverse quadratic dependence on d_{eff} [Eq. (1)], E_Z^C increases strongly as the QW width reduces. Strong fields may induce carrier tunneling out of the QW, thereby reducing the lifetime of carriers within the QW. To avoid this effect, it is advantageous to probe the SIA-BIA compensation mechanism in rather thick QWs (thickness >20 nm).

III. SAMPLE STRUCTURE AND PROCESSING

The samples were grown by molecular beam epitaxy (MBE) on n- or p-type doped GaAs(111)B substrates misoriented 2° towards the $(2\bar{1}\bar{1})$ plane. The growth temperature and rate were set to 600 °C and 0.5 μm/h, respectively. The As_4 flux was adjusted to produce the static $\sqrt{19} \times \sqrt{19}\,\text{R}\,23°$ surface reconstruction.[33–35] Under these conditions, mirror-like surfaces without pyramid-shaped features, which are often observed for growth on GaAs(111) substrates, were obtained.

In order to apply the electric control field, a stack of (111)B QWs was embedded within the intrinsic region of n-i-p or p-i-n diode structures. In these structures, the electric field induced by forward or reverse bias is oriented along the [111] or $[\bar{1}\bar{1}\bar{1}]$ direction, respectively. Figures 3(a) and 3(b) depict the layer structure for the n-i-p sample. The active region consists of 20 periods of 25 nm thick GaAs QWs separated by 31 nm thick (Al,Ga)As barriers. The nominal doping concentrations for the n- and p-type regions are $2.0 \times 10^{18}\,\text{cm}^{-3}$ and $1.2 \times 10^{18}\,\text{cm}^{-3}$, respectively. The p-i-n sample has a very similar design (not shown), apart from reversed positions of the n-type and p-type regions. To restrict the applied voltage

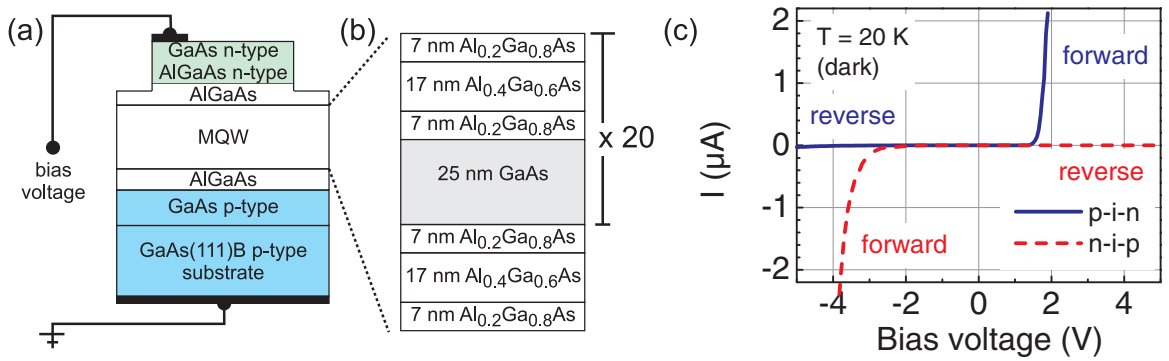

FIG. 3. (a) Layer structure of the n-i-p diodes. The MQW region is illustrated in detail in (b). (c) I-V characteristics of a p-i-n (blue, full line) and a n-i-p (red, dashed line) diode-like structure, taken in the dark at $T = 20$ K.

laterally, the top doped layers and part of the undoped AlGaAs spacer layer above the MQW stack were processed into mesa structures with a diameter of 300 μm by wet chemical etching. Schottky contacts were formed by evaporating a sequence of metallic layers [Ti (10 nm), Al (40 nm), Ti (10 nm)]. The resulting built-in potential and electric field in the structures were calculated to amount to 1.4 V and 10 kV/cm, respectively.

IV. EXPERIMENTS

The optical measurements were carried out at T = 20 K in a microscope cold finger cryostat with electric feedthroughs for bias application. Spin polarized charge carriers were generated by exciting the sample with a circularly polarized beam from a pulsed semiconductor laser (wavelength of 757 nm, pulse width and repetition rate of 150 ps and 40 MHz, respectively) impinging at normal incidence. Since the barrier layers are transparent for the laser wavelength, the carriers are generated directly in the MQW structures. The laser beam was focused onto a rather broad spot (20 μm in diameter) in order to reduce the excitation density to less than about 5 W/cm^2. The PL emitted with intensities of left (I^-) and right (I^+) circular polarization was spatially separated into two beams using a quarter-wave plate followed by a Wollaston prism. The two components were then spectrally resolved using a monochromator with a 1200 lines/mm grating and detected by charge-coupled-device cameras (CCD). We used a liquid nitrogen cooled CCD camera for cw measurements and a thermoelectrically cooled, gated one for time-resolved measurements with a resolution of about 400 ps. The gated CCD camera was synchronized with the pulsed laser using an electric delay line. The degree of spin polarization $\rho_s(t)$ was determined from the measured intensities according to $\rho_s(t) = [I^+(t) - I^-(t)]/[I^+(t) + I^-(t)]$. Since hole spins dephase on a very short time scale (typically below 0.1 ns), the PL polarization for longer times reflects the one for electron spins. The setup also includes a pair of coils outside of the cryostat, which produces an in-plane magnetic field at the sample position of up to 165 mT.

V. RESULTS AND DISCUSSION

Figure 3(c) compares the current(I)–voltage(V) characteristics of the p-i-n (blue, full line) and n-i-p (red, dashed line) structures recorded at T = 20 K in the dark. For both samples, V is defined as the potential difference between the top and the bottom contacts. Forward bias corresponds, therefore, to positive V for the p-i-n sample and negative V for the n-i-p sample. Both samples show good rectification with very low reverse currents, thus indicating that large fields can be applied under reverse biases without increasing the leakage current. In the forward direction, the p-i-n and n-i-p devices have threshold voltages of 1.7 V and −3.3 V, respectively. The origin for the difference in the absolute values of the threshold voltage is not yet clear, but might be ascribed to small deviations in doping levels as well as in the heights of the nominally identical MQW barriers in the p-i-n and n-i-p samples.

Figure 4(a) compares PL spectra for the n-i-p sample recorded at near flat-band conditions (bias voltage = −0.6 V, black solid line) as well as for reverse biases of 1.0 V (green dotted line) and 2.0 V (red dashed line). The PL line has the shortest emission wavelength (816.5 nm) and the narrowest full width at half maximum (FWHM = 4.8 meV) under flat-band conditions. Application of a reverse bias red-shifts and broadens the PL line. This behavior is attributed to the quantum confined Stark effect (QCSE) induced by the applied field [cf. Fig. 5(b)]. The maps of Fig. 4(b) show the dependence of the PL on bias. The dashed line depicts the Stark shift, which was determined by calculating the lowest eigenenergies for electron and heavy hole states in the QW structure [Fig. 3(b)] as a function of the applied bias by means of an 8-band k · p method. The ratio between the voltage drop across the MQW region and the externally applied voltage was fitted to match the experimental data. Based on the fitted Stark shift, we deduced the electric field (E) across the MQW displayed in the upper horizontal scale. The PL lines under applied bias voltage are very broad with FWHM values of up to 24 meV. One reason for the broadening might be a non-uniform electric field across the MQW region created by a redistribution of residual and photo-generated carriers, which leads to different Stark shifts for different QWs. The bias independent PL signal around λ = 833 nm stems from carbon-related radiative centers in the substrate.

The applied bias also affects the lifetimes of photo-generated carriers and the intensity of the PL emission. Figure 5 shows the carrier lifetimes deduced from time-resolved PL measurements on the n-i-p sample as a function of the

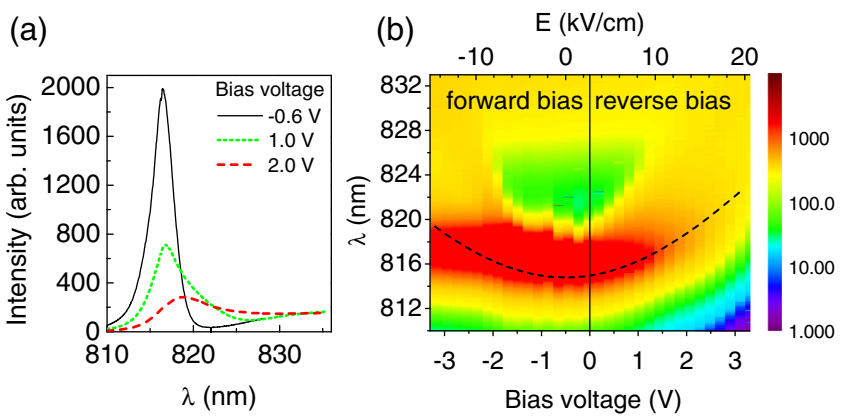

FIG. 4. (a) PL spectra recorded on a n-i-p sample at near flat band condition (V = −0.6 V, black solid line) and at reverse biases of 1.0 V (green dotted line) and 2.0 V (red dashed line). (b) PL intensity plot (in a log scale) in dependence of the bias voltage at T = 20 K. The dashed line depicts the calculated Stark shift, where the ratio of the voltage drop across the MQW region to the externally applied voltage was adjusted to fit the experimental data. The upper horizontal scale denotes the electric field (E) across the MQW determined from this fitting procedure.

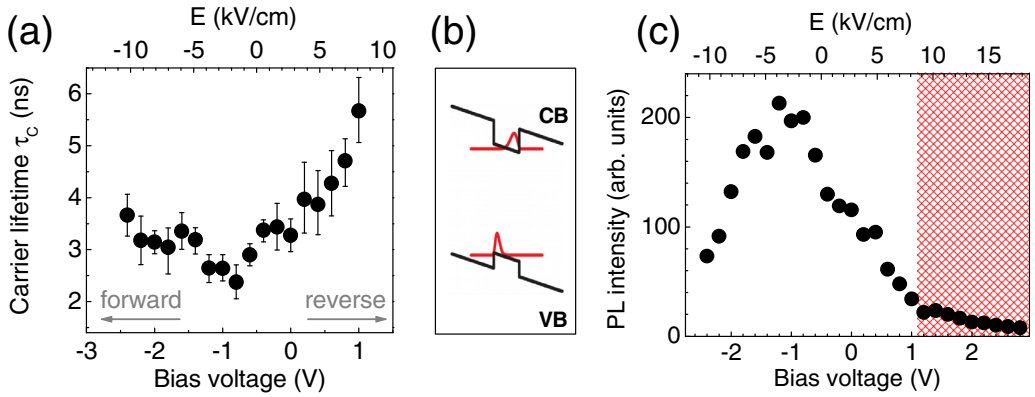

FIG. 5. (a) Lifetime of photo-generated carriers (τ_c) in a (111)GaAs MQW within a n-i-p structure as deduced from time-resolved PL measurements. (b) Band diagram illustrating the spatial separation of electron wave function in the conduction band (CB) and hole wave function in the valence band (VB) of a biased QW. (c) Integrated QW PL intensity as a function of the applied bias voltage. The hashed area marks the voltage range, where the integrated PL intensity is too low for reliable determination of the electron spin polarization using PL.

bias voltage. The carrier lifetimes increase for both forward and reverse biases. This behavior is ascribed to the spatial separation of the electron and hole wave functions [cf. Fig. 5(b)], which reduces the probability for radiative recombination. Long carrier lifetimes are necessary for the detection of long-living spins. Unfortunately, the spatial separation also significantly reduces the PL intensity, as shown in Fig. 5(c). The low PL intensity also limits the range of voltages for reliable spin polarization measurements to $V < 1.2$ V, corresponding to maximum field of 9 kV/cm in n-i-p structures. These fields are much lower than the expected value for compensation of 28 kV/cm.

The impact of the applied field on the spin dynamics is illustrated in Fig. 6. The panels on the left hand side display time-resolved profiles for the spin polarization ρ_s recorded under different applied biases. The red, full lines are fits of the profiles to a decaying exponential function used to determine the electron spin lifetime τ_s. Increasing the electric field from -9.2 kV/cm (top panel) to 8.1 kV/cm (bottom panel) leads to a strong enhancement of τ_s from 0.9 to 4.8 ns. As will be further justified below, this enhancement is attributed to the partial compensation of the SO field due to the applied reverse bias.

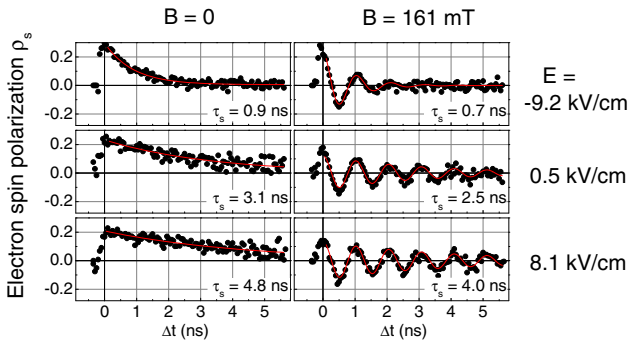

FIG. 6. Temporal evolution of the electron spin polarization ρ_s in a n-i-p GaAs(111) MQW sample in dependence of the electric field (labelling on the right hand side) measured without (left panels) and with an in-plane magnetic field of B = 161 mT (right panels). The fitting curves (full lines) correspond to single-exponential decay function (left panels) and exponentially damped cosine functions (right panels). τ_s denotes the corresponding exponential decay times.

A strong spin lifetime enhancement has also been observed under a magnetic field. The right panels show similar measurements as in the left panels in the presence of an in-plane magnetic field of B = 161 mT. The indicated spin lifetimes τ_s were determined in this case by fitting the measurements to a decaying cosine function (red, full lines). For an electric field of $E = -9.2$ kV/cm, τ_s is short and only a few spin precession oscillations occur before the spins dephase. For $E = 8.1$ kV/cm, in contrast, spin oscillations spanning over the whole range of accessible time delays can be observed.

The electron spin lifetimes measured in the n-i-p structure in the presence (red circles) and absence (black squares) of a magnetic field are compared in Fig. 7(a). The spin lifetimes increase with applied electric field and are weakly dependent on magnetic field. The last result is in fact unexpected: Since the resultant SO magnetic field is in the QW plane, the DP dephasing for out-of-plane spins should be twice as large as for in-plane ones. As a result, the spin lifetime of optically oriented spins should increase under precession. In contrast to this expectation, we observe a slight spin lifetime reduction under precession. A similar behavior was also reported by Balocchi *et al.*[24] They explain the apparent discrepancy based on the fact that higher order terms (in **k**) of the Dresselhaus contribution decrease the BIA/SIA compensation effect for spins aligned in the plane of the QW.

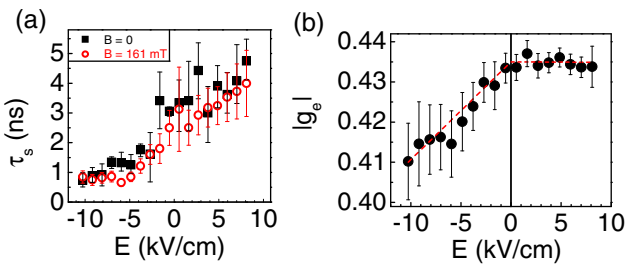

FIG. 7. (a) Electron spin lifetimes τ_s measured in n-i-p structures as a function of the electric field without (black squares) and with (red circles) an in-plane magnetic field of 161 mT. (b) Modulus of the electron g-factor in (111) QWs plotted as a function of the electric field strength E. The dashed line is a guide to the eyes.

The long spin lifetimes under precession have important consequences for applications since the spin vector can be manipulated without destroying the spin coherence. In GaAs(110) QWs, spins have long lifetime only for out-of-plane orientation and the spin polarization decays significantly as they precess around an in-plane magnetic field.[5,19] In GaAs(111) QWs, in contrast, the application of a magnetic field only slightly reduces the spin lifetime, which shows that the spin lifetime for all spin components can be electrically increased.

The fitting procedure for the determination of the spin lifetimes under a magnetic field also yields the modulus of the electron g-factor ($|g_e|$), which determines the spin oscillation frequency under the external magnetic field. The corresponding $|g_e|$ values are plotted as a function of the applied electric field in Fig. 7(b). An external field across QWs drives the electron and hole wave-functions towards the barriers [cf. Fig. 5(b)]. As the electron g-factor of AlAs and GaAs has opposite signs, the modulus of the electron g-factor is expected to decrease for an increasing applied electric field, independent of the field direction.[36] Such a behavior is indeed observed for negative fields in Fig. 7(b). Note that a non-uniform field distribution across the MQWs should also lead to a distribution of g values and of the spin precession frequencies under a magnetic field. We found, however, that the field dependence of the g-factor in Fig. 7(b) is too weak to explain the spin polarization decay in the time-resolved traces of Fig. 6. For positive fields, in contrast, g_e remains almost constant. At the moment, we cannot explain this asymmetry and further investigations have yet to be carried out.

The measurements of Figs. 4–7 were all carried out on the n-i-p diode structure, where the BIA/SIA compensation is achieved by increasing the reverse bias. For the p-i-n diode structure, in contrast, compensation requires the application of a forward bias. The range of forward biases that can be applied is, however, very limited due to current flow through the structure. In contrast, the application of a reverse bias to the p-i-n devices should increase the total SO field and reduce the spin lifetime. This expectation is in agreement with Fig. 8, which compares the electron spin lifetimes in the p-i-n (red squares) and n-i-p (blue circles) diode structures. The spin lifetimes in the figure were determined via the Hanle effect by measuring the dependence of spin polarization on an in-plane magnetic field. The modulus of the electron g-factor required for the lifetime calculations were taken from Fig. 7(b). A similar behavior of τ_s with field is observed for both types of structures. Note, in particular, that τ_s can be reduced to values below 100 ps under reverse biased p-i-n diodes.

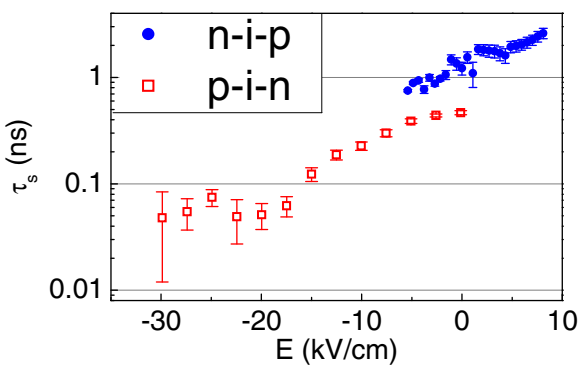

FIG. 8. Electron spin lifetimes τ_s deduced from Hanle measurements in p-i-n (red squares) and n-i-p diode structures with (111)B MQWs plotted as a function of the electric field E.

The strong reduction of τ_s under reverse bias also allows us to discard effects associated with electron-hole exchange interaction or BAP[6] spin dephasing mechanism. The BAP mechanism requires the overlap of the electron and hole wave-functions, which becomes suppressed as these functions are spatially separated under a reverse bias. Its impact on the spin lifetime in p-i-n structures is, therefore, opposite to the measured one for the p-i-n structure, thus indicating that it plays a minor role in the present experiments.

The results presented here confirm and support the findings of Balocchi *et al.*[24] Our experiments can be regarded as complementary in the following respects:

- The investigated samples contain thicker QWs. The QW thickness has a strong influence on the spin-orbit field compensation mechanism, the electron g-factor, and the quantum-confined Stark shift.
- Our experimental methods differ in that our observable maximum time span of time-resolved measurements is only restricted by the temporal evolution of the photoluminescence emission. Thus, we were able to observe several complete spin vector oscillations under an applied in-plane magnetic field.
- For comparison with theoretical works, it might be interesting that our experiments were all carried out at 20 K, whereas by Balocchi *et al.* the sample temperature was of at least 50 K.

VI. CONCLUSION

The specific symmetry of GaAs(111) QWs allows for the control of the electron spin lifetimes by using an electric field to change the relative magnitudes of the BIA and SIA contributions to the spin orbit field. In this way, the electron spin lifetimes can be changed over almost two orders of magnitude (from below 100 ps to several ns). The enhanced spin lifetimes apply for all spin wave vectors and orientations. The fact that this strategy to increase spin lifetimes was also demonstrated by Balocchi *et al.*[24] in thinner QWs at higher temperatures constitutes this BIA–SIA compensating mechanism as a generally applicable strategy to increase electron spin lifetimes in (111) III-V QWs.

The maximum spin lifetimes that could be achieved in the present experiments are limited by the resolution of the used optical techniques. Advanced time-modulated optical or pure electrical measurements are projected to evaluate the full potential of the electrical tunability of electron spin lifetimes in GaAs(111)B QWs.

ACKNOWLEDGMENTS

We thank M. Höricke, W. Seidel, and S. Rauwerdink for MBE growth and sample processing. We gratefully acknowledge financial support from the Deutsche Forschungsgemeinschaft (DFG) via the priority programme SPP1285.

[1]M. I. D'yakonov and V. I. Perel', "Spin orientation of electrons associated with the interband absorption of light in semiconductors," Sov. Phys. JETP **33**, 1053–1059 (1971).
[2]M. I. D'yakonov and V. I. Perel', "Spin relaxation of conduction electrons in noncentrosymmetric semiconductors," Sov. Phys. Solid State **13**, 3023–3026 (1972).
[3]M. I. D'yakonov and V. Y. Yu. Kachorovskii, "Spin relaxation of two-dimensional electrons in noncentrosymmetric semiconductors," Sov. Phys. Semicond. **20**, 110 (1986).
[4]R. J. Elliot, "Theory of the effect of spin orbit coupling on magnetic resonance in some semiconductors," Phys. Rev. **96**, 266 (1954).
[5]S. Döhrmann, D. Hägele, J. Rudolph, M. Bichler, D. Schuh, and M. Oestreich, "Anomalous spin dephasing in (110) GaAs quantum wells: Anisotropy and intersubband effects," Phys. Rev. Lett. **93**, 147405 (2004).
[6]G. L. Bir, A. G. Aronov, and G. E. Pikus, "Spin relaxation of electrons due to scattering by holes," Sov. Phys. JETP **42**, 705 (1976).
[7]M. Z. Maialle, E. A. de Andrada e Silva, and L. J. Sham, "Exciton spin dynamics in quantum wells," Phys. Rev. B **47**, 15776 (1993).
[8]P. H. Song and K. W. Kim, "Spin relaxation of conduction electrons in bulk III-V semiconductors," Phys. Rev. B **66**, 035207 (2002).
[9]J. M. Kikkawa, I. P. Smorchkova, N. Samarth, and D. D. Awschalom, "Room-temperature spin memory in two-dimensional electron gases," Science **277**(5330), 1284–1287 (1997).
[10]J. M. Kikkawa and D. D. Awschalom, "Resonant spin amplification in n-type GaAs," Phys. Rev. Lett. **80**, 4313 (1998).
[11]C.-H. Chang, A. G. Mal'shukov, and K. A. Chao, "Spin relaxation dynamics of quasiclassical electrons in ballistic quantum dots with strong spin-orbit coupling," Phys. Rev. B **70**, 245309 (2004).
[12]S. Pramanik, S. Bandyopadhyay, and M. Cahay, "Spin transport in nanowires," in *2003 Third IEEE Conference on Nanotechnology* (IEEE, 2003), Vol. 2, pp. 87–90.
[13]A. W. Holleitner, V. Sih, R. C. Myers, A. C. Gossard, and D. D. Awschalom, "Suppression of spin relaxation in submicron InGaAs wires," Phys. Rev. Lett. **97**, 036805 (2006).
[14]J. A. H. Stotz, R. Hey, P. V. Santos, and K. H. Ploog, "Spin transport and manipulation by mobile potential dots in GaAs quantum wells," Physica E **32**(1-2), 446 (2006).
[15]J. A. H. Stotz, R. Hey, and P. V. Santos, "Temperature dependence of spin transport by dynamic quantum dots," Mater. Sci. Eng., B **126**, 164–167 (2006).
[16]Y. Ohno, R. Terauchi, T. Adachi, F. Matsukura, and H. Ohno, "Spin relaxation in GaAs(110) quantum wells," Phys. Rev. Lett. **83**, 4196–4199 (1999).
[17]O. D. D. Couto, Jr., F. Iikawa, J. Rudolph, R. Hey, and P. V. Santos, "Anisotropic spin transport in (110) GaAs quantum wells," Phys. Rev. Lett. **98**, 036603 (2007).
[18]G. M. Müller, M. Römer, D. Schuh, W. Wegscheider, J. Hübner, and M. Oestreich, "Spin noise spectroscopy in GaAs (110) quantum wells: Access to intrinsic spin lifetimes and equilibrium electron dynamics," Phys. Rev. Lett. **101**(20), 206601 (2008).
[19]S. Iba, S. Koh, and H. Kawaguchi, "Room temperature gate modulation of electron spin relaxation time in (110)-oriented GaAs/AlGaAs quantum wells," Appl. Phys. Lett. **97**, 202102 (2010).
[20]K. Biermann, O. D. D. Couto, Jr., E. Cerda, H. B. de Carvalho, R. Hey, and P. V. Santos, "Spin transport in (110) GaAs-based cavity structures," J. Supercond. Novel Magn. **23**, 27 (2010).
[21]X. Cartoixa, D. Z.-Y. Ying, and Y.-C. Chang, "Suppression of the D'yakonov-Perel' spin-relaxation mechanism for all spin components in 111] zincblende quantum wells," Phys. Rev. B **71**, 045313 (2005).
[22]I. Vurgaftman and J. R. Meyer, "Spin-relaxation suppression by compensation of bulk and structural inversion asymmetries in [111]-oriented quantum wells," J. Appl. Phys. **97**(5), 053707 (2005).
[23]B. Y. Sun, P. Zhang, and M. W. Wu, "Spin relaxation in n-type (111) GaAs quantum wells," J. Appl. Phys. **108**, 093709 (2010).
[24]A. Balocchi, Q. H. Duong, P. Renucci, B. L. Liu, C. Fontaine, T. Amand, D. Lagarde, and X. Marie, "Full electrical control of the electron spin relaxation in GaAs quantum wells," Phys. Rev. Lett. **107**, 136604 (2011).
[25]J. Schliemann, J. C. Egues, and D. Loss, "Nonballistic spin-field-effect transistor," Phys. Rev. Lett. **90**, 146801 (2003).
[26]N. S. Averkiev and L. E. Golub, "Giant spin relaxation anisotropy in zinc-blende heterostructures," Phys. Rev. B **60**, 15582–15584 (1999).
[27]N. S. Averkiev, L. E. Golub, A. S. Gurevich, V. P. Evtikhiev, V. P. Kochereshko, A. V. Platonov, A. S. Shkolnik, and Yu. P. Efimov, "Spin-relaxation anisotropy in asymmetrical (001) $Al_xGa_{1-x}As$ quantum wells from Hanle-effect measurements: Relative strengths of Rashba and Dresselhaus spin-orbit coupling," Phys. Rev. B **74**, 033305 (2006).
[28]V. Lechner, L. E. Golub, P. Olbrich, S. Stachel, D. Schuh, W. Wegscheider, V. V. Belkov, and S. D. Ganichev, "Tuning of structure inversion asymmetry by the δ-doping position in (001)-grown GaAs quantum wells," Appl. Phys. Lett. **94**, 242109 (2009).
[29]O. D. D. Couto, Jr., R. Hey, and P. V. Santos, "Spin dynamics in (110) GaAs quantum wells under surface acoustic waves," Phys. Rev. B **78**, 153305 (2008).
[30]R. Winkler, *Spin-Orbit Coupling Effects in Two-Dimensional Electron and Hole Systems* (Springer, Berlin, 2003), Vol. 191.
[31]D. Richards, B. Jusserand, H. Peric, and B. Etienne, "Intrasubband excitations and spin-splitting anisotropy in GaAs modulation-doped quantum wells," Phys. Rev. B **47**, 16028–16031 (1993).
[32]P. S. Eldridge, W. J. H. Leyland, P. G. Lagoudakis, O. Z. Karimov, M. Henini, D. Taylor, R. T. Phillips, and R. T. Harley, "All-optical measurement of Rashba coefficient in quantum wells," Phys. Rev. B **77**, 125344 (2008). (Their defined Rashba coefficient α corresponds to 2 r_{41}, as it is used here.)
[33]A. Y. Cho, "Morphology of epitaxial growth of GaAs by a molecular beam method: The observation of surface structures," J. Appl. Phys. **41**, 2780–2786 (1970).
[34]D. A. Woolf, Z. Sobiesierski, D. I. Westwoood, and R. H. Williams, "The molecular beam epitaxial growth of GaAs/GaAs(111)B: Doping and growth temperature studies," J. Appl. Phys. **71**, 4908–4915 (1992).
[35]D. A. Woolf, D. I. Westwoood, and R. H. Williams, "The homoepitaxial growth of GaAs(111)A and GaAs(111)B by molecular beam epitaxy: An investigation of the temperature-dependent surface reconstructions and bulk electrical conductivity transitions," Semicond. Sci. Technol. **8**, 1075–1081 (1993).
[36]I. A. Yugova, A. Greilich, D. R. Yakovlev, A. A. Kiselev, M. Bayer, V. V. Petrov, Yu. K. Dolgikh, D. Reuter, and A. D. Wieck, "Universal behavior of the electron g factor in GaAs/$Al_xGa_{1-x}As$ quantum wells," Phys. Rev. B **75**, 245302 (2007).